

The Kaon B -parameter in Mixed Action Chiral Perturbation Theory

C. Aubin,^{1,*} Jack Laiho,^{2,†} and Ruth S. Van de Water^{2,‡}

¹*Department of Physics, Columbia University, New York, NY 10027*

²*Theoretical Physics Department, Fermilab, Batavia, IL 60510*

(Dated: December 24, 2018)

Abstract

We calculate the kaon B -parameter, B_K , in chiral perturbation theory for a partially quenched, mixed action theory with Ginsparg-Wilson valence quarks and staggered sea quarks. We find that the resulting expression is similar to that in the continuum, and in fact has only two additional unknown parameters. At one-loop order, taste-symmetry violations in the staggered sea sector only contribute to flavor-disconnected diagrams by generating an $\mathcal{O}(a^2)$ shift to the masses of taste-singlet sea-sea mesons. Lattice discretization errors also give rise to an analytic term which shifts the tree-level value of B_K by an amount of $\mathcal{O}(a^2)$. This term, however, is not strictly due to taste-breaking, and is therefore also present in the expression for B_K for pure G-W lattice fermions. We also present a numerical study of the mixed B_K expression in order to demonstrate that both discretization errors and finite volume effects are small and under control on the MILC improved staggered lattices.

PACS numbers: 11.15.Ha, 12.39.Fe, 12.38.Gc

*caubin@phys.columbia.edu

†jlaiho@fnal.gov

‡ruthv@fnal.gov

I. INTRODUCTION

Lattice quantum chromodynamics allows nonperturbative calculations of low-energy QCD quantities from first principles. Until recently, limited computing resources and the inability to include quark loop effects have prevented lattice calculations from achieving realistic results. In the past few years, however, lattice simulations of both light meson and heavy-light meson quantities with dynamical staggered quarks have shown excellent numerical agreement with experimental results [1]. These have included both post-dictions, such as the pion and kaon decay constants [2], and predictions, as in the case of the B_c meson mass [3]. Such successes demonstrate that many of the systematic uncertainties associated with lattice simulations are under control, and therefore give confidence that lattice simulations can reliably calculate quantities that cannot be accessed experimentally. One of the simplest quantities of phenomenological importance that can only be calculated using lattice QCD is the kaon B-parameter, B_K . Thus a precise measurement of B_K is an important goal for the lattice community.¹

B_K parameterizes the hadronic contribution to $K^0 - \bar{K}^0$ mixing; it therefore plays a crucial role in extracting information about the CKM matrix using measurements of the neutral kaon system. In particular, the size of indirect CP violation in the neutral kaon system, ϵ_K , when combined with a numerical value for B_K , places an important constraint on the apex of the CKM unitarity triangle [7, 8]. Because ϵ_K is well known experimentally [9], the dominant source of error in this procedure is the uncertainty in the lattice determination of B_K . It is likely that new physics would give rise to CP-violating phases in addition to that of the CKM matrix; such phases would manifest themselves as apparent inconsistencies among different measurements of quantities which should be identical within the standard CKM picture. Thus a precise determination of B_K will help to constrain physics beyond the standard model.

Because lattice simulations with staggered fermions can at present reach significantly lighter quark masses than those with other standard discretizations [10, 11], calculations of weak matrix elements using the available 2+1-flavor Asqtad staggered lattices appear promising. Unfortunately, however, one pays a significant price for the computational speed

¹ Promising calculations of B_K including dynamical quark effects are currently in progress using both improved staggered fermions [4, 5] and domain-wall fermions [6].

of staggered simulations: each flavor of staggered quark comes in four species, or “tastes.” In the continuum limit, these species become degenerate and can be removed by taking the fourth root of the fermion determinant. In practice, however, one must take the fourth root of the quark determinant during the lattice simulation in order to remove the extra tastes; thus it is an open theoretical question whether or not one recovers QCD after taking the continuum limit of fourth-rooted lattice simulations.² In this paper we assume the validity of the fourth-root trick. Even working under this assumption, however, the additional tastes introduce complications to staggered lattice simulations. The degeneracy among the four tastes is broken by the nonzero lattice spacing, a , and results in discretization errors of $\mathcal{O}(a^2)$. Thus one must use functional forms calculated in staggered chiral perturbation theory (S χ PT), in which taste-violating effects are explicit, to correctly extrapolate staggered lattice data [16, 17, 18, 19].

Staggered chiral perturbation theory has been used to successfully fit quantities such as f_π and f_D , for which the S χ PT expressions are simple and taste-symmetry breaking primarily enters through additive corrections to the pion masses inside loops [18, 20]. In the case of B_K , however, the additional tastes also make the matching procedure between the lattice $\Delta S = 2$ effective four-fermion operator and the desired continuum operator more difficult. The latticized version of the continuum B_K operator mixes with all other lattice operators that are in the same representation of the staggered lattice symmetry group [21] – including those with different tastes than the valence mesons. Current staggered calculations only account for mixing with operators of the correct taste and only to 1-loop order in α_S ; this results in a 20% uncertainty in B_K [4]. In order to achieve a precise determination of B_K with staggered fermions, one must either perform the lattice-to-continuum matching nonperturbatively using a method such as that of the Rome-Southampton group [22] or one must include the effects of the extra operators in the S χ PT expression for B_K [23]. Thus far the large number of staggered operators has prevented matching calculations beyond 1-loop order [24, 25], although nonperturbative matching including all relevant staggered operators is, in principle, possible. The effects of this truncated lattice-to-continuum operator matching can be included in an extended version of S χ PT, but the resulting expression for B_K has

² Recently several papers have appeared addressing the validity of the fourth-root trick. We refer the reader to Refs. [12, 13, 14, 15] and the references therein for a sampling of the available literature.

37 undetermined fit parameters, only 5 of which are already known from measurements of other quantities. Therefore use of this expression may prove just as difficult as implementing fully nonperturbative matching.

The calculation of weak matrix elements such as B_K with Ginsparg-Wilson (G-W) quarks [26], on the other hand, is theoretically much cleaner than that with staggered quarks. This is because in the massless limit, G-W quarks possess an exact chiral symmetry on the lattice and do not occur in multiple species. Although in practice, lattice simulations use approximate G-W fermions, the degree to which chiral symmetry is broken in simulations can be controlled either by the length of the fifth dimension in the case of domain-wall quarks [27, 28] or through the degree to which the overlap operator is realized in the case of overlap quarks [29, 30, 31]. Consequently, while the $\Delta S = 2$ lattice operator still mixes with wrong-chirality operators, there are significantly fewer operators than in the staggered case, and nonperturbative renormalization can be used in the determination of B_K . As an additional benefit, the approximate chiral symmetry also ensures that the appropriate chiral perturbation theory expression for use in the extrapolation of B_K lattice data is continuum-like at next-to-leading order (NLO). Lattice simulations with G-W fermions, however, are 10 to 100 times more computationally expensive than those with staggered fermions with comparable masses and lattice spacing, and thus are unfortunately not yet practical for realizing light dynamical quark masses.

A computationally affordable compromise is therefore to calculate correlation functions with G-W valence quarks on a background of dynamical staggered gauge configurations. This “mixed action” procedure takes advantage of the best properties of both discretizations. By using staggered sea quarks and domain-wall valence quarks one can better approach the chiral regime in the sea sector while minimizing operator mixing and allowing the use of nonperturbative renormalization. Additionally, because the MILC staggered lattices with 2+1 flavors of dynamical quarks are publicly available and offer a number of quark masses and lattice spacings [10, 11], one can perform mixed-action simulations at the same cost as quenched G-W simulations. Mixed action simulations have already been successfully used to study quantities of interest to nuclear physics [32, 33], thus we expect that a similar method can be used to calculate the weak matrix element B_K . Moreover, we believe that this proposed mixed-action method is the best way to determine B_K both precisely and in a timely manner, thereby producing the largest phenomenological impact.

One might be concerned that the use of a mixed action could introduce new theoretical complications into the lattice determination of B_K . This is not, however, the case. Although the mixed staggered sea, G-W valence lattice theory reduces to QCD in the continuum limit, at nonzero lattice spacing, it is manifestly unphysical in that it violates unitarity. Thus, in order to extract physical QCD quantities from mixed action simulations, it is essential that one can correctly describe and remove contributions due to unphysical mixed action effects from quantities such as B_K using the appropriate lattice chiral perturbation theory. It has not been rigorously proven that the mixed action chiral perturbation theory developed in [34] is the correct chiral effective theory for mixed G-W, staggered simulations in which the fourth-root of the quark determinant is taken in the sea sector. Nevertheless, Ref. [34] showed that, given a small number of plausible assumptions, staggered chiral perturbation theory is the correct chiral effective theory for describing the pseudo-Goldstone boson sector of rooted staggered simulations. A similar line of reasoning should follow for mixed action chiral perturbation theory. Consequently, mixed action lattice simulations can be used to correctly calculate quantities involving pseudo-Goldstone bosons (such as B_K) in QCD. More complicated quantities, however, should be considered on a case-by-case basis.

In this paper we calculate B_K in χ PT for a lattice theory with G-W valence quarks and staggered sea quarks. We present results for a “1+1+1” theory in which $m_u \neq m_d \neq m_s$ in the sea sector, for a “2+1” theory in which $m_u = m_d \neq m_s$ in the sea sector, and for a “full QCD”-like expression in which we tune the valence-valence meson masses equal to the taste-singlet sea-sea meson masses. (We emphasize, however, that these expressions only truly reduce to QCD when $m_{\text{sea}} = m_{\text{valence}}$ and the lattice spacing $a \rightarrow 0$.) These expressions will be necessary for the correct chiral and continuum extrapolation of mixed-action B_K lattice data. We find that the expression for B_K in mixed action χ PT has only two more parameters than in the continuum. The first coefficient multiplies an analytic term which shifts the tree-level value of B_K by an amount of $\mathcal{O}(a^2)$; this term is also present in the case of pure G-W lattice fermions. The second new parameter shifts the mass of the taste-singlet sea-sea meson (which only appears inside loop diagrams) by an amount of $\mathcal{O}(a^2)$. This mass-splitting has already been separately determined, however, in the MILC spectrum calculations so we do not consider it to be an unknown fit parameter. Therefore, in practice, the chiral and continuum extrapolation of mixed action B_K lattice data should be

no more complicated than that of domain-wall lattice data. A numerical analysis using the taste-breaking parameters measured on the MILC coarse lattices ($a \approx 0.125$ fm) shows that the size of non-analytic discretization errors should be less than a percent of the continuum value of B_K over the relevant extrapolation range. In addition, we find that finite volume effects in B_K are also small, and are of $\mathcal{O}(1\%)$ for the lightest pion mass on the MILC coarse ensemble.

This paper is organized as follows. We review mixed action chiral perturbation theory (MAXPT) in Sec. II. In Sec. III we calculate B_K to next-to-leading order in MAXPT. This is divided into four subsections: we first present the spurion analysis necessary to map the quark-level B_K operator onto an operator in the chiral effective theory in Sec. III A, calculate the 1-loop contributions to B_K at NLO in Sec. III B, determine the analytic contributions to B_K at NLO in Sec. III C, and finally present the complete expressions for B_K at NLO in MAXPT in Sec. III D. Next, in Sec. IV, we estimate the numerical size of both taste-symmetry breaking contributions and finite volume effects on the existing MILC ensembles using the resulting mixed action χ PT formulae. Finally, we conclude in Sec. V.

II. MIXED ACTION CHIRAL PERTURBATION THEORY

In this section we review the leading-order mixed action chiral Lagrangian, first determined in Ref. [34], and discuss some of its physical consequences for the pseudo-Goldstone boson sector.

We consider a partially quenched theory with N_{val} Ginsparg-Wilson valence quarks and N_{sea} staggered sea quarks. Each staggered sea quark comes in four tastes, and each G-W valence quark has a corresponding bosonic ghost partner to cancel its contribution to loop diagrams. For example, in the case $N_{\text{val}} = 2$ and $N_{\text{sea}} = 3$, the quark mass matrix is given by

$$M = \text{diag}(\underbrace{m_u, m_u, m_u, m_u, m_d, m_d, m_d, m_d, m_s, m_s, m_s, m_s}_{\text{sea}}, \underbrace{m_x, m_y, m_x, m_y}_{\text{valence}}, \underbrace{m_x, m_y}_{\text{ghost}}), \quad (1)$$

where we label the dynamical quarks by u , d , and s and the valence quarks by x and y . The mixed action theory has an approximate $SU(4N_{\text{sea}} + N_{\text{val}}|N_{\text{val}})_L \otimes SU(4N_{\text{sea}} + N_{\text{val}}|N_{\text{val}})_R$ graded chiral symmetry which becomes exact in the combined massless quark and continuum limit. In analogy with QCD, we assume that chiral symmetry spontaneously breaks to its

vector subgroup,

$$SU(4N_{\text{sea}} + N_{\text{val}}|N_{\text{val}})_L \otimes SU(4N_{\text{sea}} + N_{\text{val}}|N_{\text{val}})_R \xrightarrow{SSB} SU(4N_{\text{sea}} + N_{\text{val}}|N_{\text{val}})_V, \quad (2)$$

and gives rise to $(4N_{\text{sea}} + 2N_{\text{val}})^2 - 1$ pseudo-Goldstone bosons (PGBs). These PGBs can be packaged in an $SU(4N_{\text{sea}} + N_{\text{val}}|N_{\text{val}})$ matrix:

$$\Sigma = \exp\left(\frac{2i\Phi}{f}\right), \quad \Phi = \begin{pmatrix} U & \pi^+ & K^+ & Q_{ux} & Q_{uy} & \cdots & \cdots \\ \pi^- & D & K^0 & Q_{dx} & Q_{dy} & \cdots & \cdots \\ K^- & \bar{K}^0 & S & Q_{sx} & Q_{sy} & \cdots & \cdots \\ Q_{ux}^\dagger & Q_{dx}^\dagger & Q_{sx}^\dagger & X & P^+ & R_{xx}^\dagger & R_{\tilde{y}x}^\dagger \\ Q_{uy}^\dagger & Q_{dy}^\dagger & Q_{sy}^\dagger & P^- & Y & R_{\tilde{x}y}^\dagger & R_{\tilde{y}y}^\dagger \\ \cdots & \cdots & \cdots & R_{\tilde{x}x} & R_{\tilde{x}y} & \tilde{X} & \tilde{P}^+ \\ \cdots & \cdots & \cdots & R_{\tilde{y}x} & R_{\tilde{y}y} & \tilde{P}^- & \tilde{Y} \end{pmatrix}, \quad (3)$$

where f is normalized such that $f_\pi \approx 131$ MeV. The upper-left block of Φ contains sea-sea PGBs, each of which comes in sixteen tastes. For example,

$$U = \sum_{b=1}^{16} U_b \frac{T_b}{2}, \quad (4)$$

where the Euclidean gamma matrices

$$T_b = \{\xi_5, i\xi_\mu\xi_5, i\xi_\mu\xi_\nu, \xi_\mu, \xi_I\} \quad (5)$$

are the generators of the continuum $SU(4)$ taste symmetry (ξ_I is the 4×4 identity matrix). The fields in the central block are the flavor-charged (P^+ and P^-) and flavor-neutral (X and Y) valence-valence PGBs, while those in the lower-right block with tildes are the analogous PGBs composed of only ghost quarks. Finally, the off-diagonal blocks contain “mixed” PGBs: those labeled by R ’s are composed of one valence and one ghost quark, while those labeled by Q ’s are composed of one valence and one sea quark. We do not show the mixed ghost-sea PGBs explicitly; their locations are indicated by ellipses.

Under chiral symmetry transformations, Σ transforms as

$$\Sigma \longrightarrow L \Sigma R^\dagger, \quad L, R \in SU(4N_{\text{sea}} + N_{\text{val}}|N_{\text{val}})_{L,R}. \quad (6)$$

The standard mixed action chiral perturbation theory power-counting scheme is

$$p_{\text{PGB}}^2/\Lambda_\chi^2 \sim m_q/\Lambda_{\text{QCD}} \sim a^2 \Lambda_{\text{QCD}}^2, \quad (7)$$

so the lowest-order, $\mathcal{O}(p_{\text{PGB}}^2, m_q, a^2)$, mixed action chiral Lagrangian is

$$\mathcal{L} = \frac{f^2}{8} \text{Str}(\partial_\mu \Sigma \partial_\mu \Sigma^\dagger) - \frac{\mu f^2}{4} \text{Str}(\Sigma M^\dagger + M \Sigma^\dagger) + a^2 (\mathcal{U}_S + \mathcal{U}'_S + \mathcal{U}_V), \quad (8)$$

where Str indicates a graded supertrace over both flavor and taste indices and μ is an undetermined dimensionful parameter of $\mathcal{O}(\Lambda_{\text{QCD}})$. The leading-order expression for the mass-squared of a valence-valence PGB is identical to that of the continuum because the chiral symmetry of the valence sector prevents an additive shift due to lattice spacing effects:

$$m_{xy}^2 = \mu(m_x + m_y). \quad (9)$$

\mathcal{U}_S and \mathcal{U}'_S comprise the well-known staggered potential and come from taste-symmetry breaking in the sea quark sector [17]. \mathcal{U}_S splits the tree-level masses of the sea-sea PGBs into degenerate groups:

$$m_{ff',t}^2 = \mu(m_f + m_{f'}) + a^2 \Delta_t, \quad (10)$$

where Δ_t is different for each of the $SO(4)$ -taste irreps: P, V, A, T, I . In particular, $\Delta_P = 0$ because the taste-pseudoscalar sea-sea PGB is a true lattice Goldstone boson. The mixed action Lagrangian contains only one new operator, and thus one new low-energy constant, as compared to the staggered chiral Lagrangian:

$$\mathcal{U}_V = -C_{\text{Mix}} \text{Str}(\tau_3 \Sigma \tau_3 \Sigma^\dagger), \quad (11)$$

where

$$\tau_3 = P_{\text{sea}} - P_{\text{val}} = \text{diag}(I_{\text{sea}} \otimes I_{\text{taste}}, -I_{\text{val}}, -I_{\text{val}}). \quad (12)$$

This operator links the valence and sea sectors and generates a shift in the mass-squared of a mixed valence-sea PGB:

$$m_{fx}^2 = \mu(m_f + m_x) + a^2 \Delta_{\text{Mix}}, \quad \Delta_{\text{Mix}} = \frac{16C_{\text{Mix}}}{f^2}. \quad (13)$$

Although the parameter Δ_{Mix} has not yet been calculated in mixed action lattice simulations, it can, in principle, be determined by calculating the mass of a mixed valence-sea meson on the lattice. As in any partially quenched theory, the mixed action theory contains flavor-neutral quark-disconnected hairpin propagators which have double pole contributions. The only flavor-neutral propagators that appear in the expression for B_K are those with two valence quarks; these have the following form:

$$G_{XY}(q) = \frac{\delta_{XY}}{q^2 + m_X^2} + D_{XY}(q), \quad (14)$$

where

$$D_{XY}(q) = -\frac{1}{3} \frac{1}{(q^2 + m_X^2)(q^2 + m_Y^2)} \frac{(q^2 + m_{U_I}^2)(q^2 + m_{D_I}^2)(q^2 + m_{S_I}^2)}{(q^2 + m_{\pi_I^0}^2)(q^2 + m_{\eta_I}^2)} \quad (15)$$

is the disconnected (hairpin) contribution. Note that the sea-sea PGBs in the above expression are all taste singlets because the valence quarks do not transform under the taste symmetry.

III. B_K AT NLO IN MIXED ACTION CHIRAL PERTURBATION THEORY

In this section we outline the calculation of B_K in mixed action χ PT. We divide it into four subsections. We first determine the operators that contribute to B_K in the mixed action chiral effective theory using a spurion analysis in Sec. III A. In Sec. III B we outline the 1-loop calculation of B_K , and in Sec. III C we follow this up with an enumeration of the corresponding analytic terms. Finally, the complete NLO results are presented in Sec. III D.

A. B_K Spurion Analysis

The spurion analysis for B_K in the mixed action case is similar to that in the continuum [23, 35]; we will point out differences when they occur.

In continuum QCD, B_K is defined as a ratio of matrix elements:

$$B_K \equiv \frac{\mathcal{M}_K}{\mathcal{M}_{\text{vac}}} . \quad (16)$$

The numerator in the above expression measures the hadronic contribution to neutral kaon mixing:

$$\mathcal{M}_K = \langle \bar{K}^0 | \mathcal{O}_K | K^0 \rangle, \quad (17)$$

$$\mathcal{O}_K = [\bar{s}\gamma_\mu(1 - \gamma_5)d][\bar{s}\gamma_\mu(1 - \gamma_5)d], \quad (18)$$

where we have dropped color indices in \mathcal{O}_K because both color contractions give rise to the same operators in the chiral effective theory. \mathcal{O}_K is an electroweak operator which transforms as a $(27_L, 1_R)$ under the standard continuum chiral symmetry group. The denominator in Eq. (16) is the same matrix element as in the numerator evaluated in the vacuum saturation approximation:

$$\mathcal{M}_K^{\text{vac}} = \frac{8}{3} \langle \bar{K}^0 | \bar{s}\gamma_\mu(1 - \gamma_5)d | 0 \rangle \langle 0 | \bar{s}\gamma_\mu(1 - \gamma_5)d | K^0 \rangle, \quad (19)$$

so that B_K is normalized to be of $\mathcal{O}(1)$.

In the mixed action theory, we define B_K in an analogous manner, except that both the external kaons and the operator \mathcal{O}_K must now be composed of valence quarks:

$$\mathcal{O}_K^{\text{lat}} = [\bar{y}\gamma_\mu(1 - \gamma_5)x][\bar{y}\gamma_\mu(1 - \gamma_5)x]. \quad (20)$$

We can rewrite this operator as follows:

$$\mathcal{O}_K^{\text{lat}} = 4[\bar{q}_L(\gamma_\mu \otimes P_{\bar{y}x})q_L][\bar{q}_L(\gamma_\mu \otimes P_{\bar{y}x})q_L], \quad (21)$$

where the subscript “ L ” on the quark field indicates the left-handed projection and the matrix $P_{\bar{y}x}$ is a $4N_{\text{sea}} + 2N_{\text{val}}$ matrix in flavor space that projects out the $\bar{y}x$ component of each quark bilinear ($[P_{\bar{y}x}]_{ij} = \delta_{i,14}\delta_{j,13}$ for $N_{\text{sea}} = 3$, $N_{\text{val}} = 2$). If we promote $P_{\bar{y}x}$ to a spurion field, F_K , which can transform under the mixed action chiral symmetry group $SU(4N_{\text{sea}} + N_{\text{val}}|N_{\text{val}})_L \otimes SU(4N_{\text{sea}} + N_{\text{val}}|N_{\text{val}})_R$, then F_K must transform as

$$F_K \rightarrow L F_K L^\dagger, \quad (22)$$

so that Eq. (21) remains invariant. One cannot build a chirally invariant operator out of Σ and the spurion field F_K without derivatives, but one can build two such operators at $\mathcal{O}(p_{\text{PGB}}^2)$:

$$\sum_\mu \text{Str}[\Sigma \partial_\mu \Sigma^\dagger F_K] \text{Str}[\Sigma \partial_\mu \Sigma^\dagger F_K], \quad (23)$$

$$\sum_\mu \text{Str}[\Sigma \partial_\mu \Sigma^\dagger F_K \Sigma \partial_\mu \Sigma^\dagger F_K]. \quad (24)$$

It turns out however, that these two operators are equivalent when one demotes the spurion F_K to the matrix $P_{\bar{y}x}$. Thus we are left with a single chiral operator:

$$\mathcal{O}_K^\chi = \sum_\mu \text{Str}[\Sigma \partial_\mu \Sigma^\dagger P_{\bar{y}x}] \text{Str}[\Sigma \partial_\mu \Sigma^\dagger P_{\bar{y}x}]. \quad (25)$$

This operator is identical in form to the continuum B_K operator [35], but Σ contains more fields and the standard trace has been promoted to a supertrace.

Because this operator is of $\mathcal{O}(p_{\text{PGB}}^2)$, operators of $\mathcal{O}(m_q)$ and $\mathcal{O}(a^2)$, if present, could also potentially contribute at the same order in χ PT. Recall that the quark mass matrix, when promoted to a spurion field, must transform as $M \rightarrow LMR^\dagger$; thus we cannot form a chiral operator with a single power of M and two powers of F_K that is invariant under the

chiral symmetry. This is, of course, to be expected because the chiral symmetry of the G-W valence sector and the $U(1)_A$ symmetry of the staggered sea sector are sufficient to prevent any new operators involving the quark mass matrix at leading order in the chiral expansion. New operators of $\mathcal{O}(a^2)$ that are not present in the continuum can also potentially appear and contribute to B_K . As discussed in Ref. [23], such operators arise in two distinct ways: mixing with higher-dimension operators and insertions of four-fermion operators from the action. We demonstrate that these operators do not introduce taste-symmetry breaking, and therefore give rise to the same kinds of analytic terms as in the pure G-W case.

Although the B_K lattice operator is dimension 6, at the level of the Symanzik effective theory, it maps onto all continuum effective operators of dimensions 6 and higher that respect the same lattice symmetries. Operators of dimension 7 and 8 are explicitly suppressed relative to the dimension 6 B_K Symanzik effective operator by powers of a and a^2 , respectively, and can therefore be mapped onto chiral operators that may contribute to B_K at NLO. Because, however, the lattice symmetry group includes taste transformations under which the valence quarks are singlets, only dimension 7 and 8 operators composed of four valence quarks can possibly respect the same lattice symmetries as the B_K lattice operator. Moreover, the chiral symmetry of the G-W valence quarks in the B_K operator prohibits strictly valence dimension 7 four-fermion operators. Thus we need only consider dimension 8 Symanzik effective operators for the B_K operator which contain four valence quarks. Fortunately we need not enumerate all possible dimension 8 quark-level operators in order to determine all possible chiral operators of $\mathcal{O}(a^2)$ onto which they map. Because the B_K lattice operator has a L - L chiral structure, and chiral symmetry is respected by the valence sector of the lattice theory, it can only mix with higher-dimension operators that also have a L - L structure. Consequently, these operators will generate the same spurions as the dimension 6 B_K operator, and thus lead to the same chiral operator as in Eq. (25), but with an additional undetermined coefficient of $\mathcal{O}(a^2)$. At NLO in χ PT, this will simply lead to an $\mathcal{O}(a^2)$ correction to the tree-level value of B_K , which we can absorb into an analytic term. We emphasize that, although this contribution is proportional to a^2 , it is not due to taste-symmetry breaking in the staggered sea sector. Because it arises from strictly valence four-fermion operators, it is also present in simulations with pure G-W lattice fermions.

New operators that contribute to B_K at $\mathcal{O}(a^2)$ can also be produced by inserting a dimension 6 $\mathcal{O}(a^2)$ operator from the Symanzik action into the B_K four-fermion operator.

A method for combining four-fermion operators at the chiral level was developed in Ref. [19] for the purpose of determining the NLO staggered chiral Lagrangian. This method was later used in Ref. [23] to enumerate the operators that arise from insertions of the staggered action that contribute to B_K with both staggered sea and valence quarks. It is easy to map the operators given in Table III of Ref. [23], which come from insertions of taste-breaking four-fermion operators, onto the corresponding operators in the mixed-action theory: because only the staggered sea quarks in the mixed-action theory carry taste quantum numbers, simply place a matrix that projects onto the sea sector next to every taste matrix, i.e. let $\xi \rightarrow \xi \mathcal{P}_{\text{sea}}$ for each taste matrix ξ . It is then straightforward to show that all the resulting operators either vanish identically because $\mathcal{P}_{\text{sea}} P_{\bar{y}x} = 0$ or do not contribute to B_K at NLO because they have the incorrect flavor structure. The spurions that correspond to strictly valence four-fermion operators or mixed valence-sea four-fermion operators in the Symanzik action are given in Ref. [34]. Thus one can use a similar procedure to that in Ref. [23] to enumerate all of the chiral operators in the mixed-action theory that come from insertions of these four-fermion operators into the B_K operator. It turns out that all of the operators are either trivial because the matrix which projects onto the valence sector is sandwiched between Σ and Σ^\dagger or again they do not have the right flavor structure to contribute to B_K at NLO. Consequently, operators of $\mathcal{O}(a^2)$ that arise from insertions of four-fermion operators in the Symanzik effective action do not contribute to B_K at NLO for the mixed G-W, staggered lattice theory.

The previous analysis holds for G-W valence quarks, which have perfect chiral symmetry. On the lattice however, G-W quarks are often approximated as domain-wall quarks, which have a small amount of residual chiral symmetry breaking due to the finite size of the fifth dimension. This chiral symmetry breaking is parameterized by the residual mass, m_{res} , which is a measure of how far the left- and right-handed components of the quarks extend into the fifth dimension. These effects can be readily added to the chiral theory, as seen in Refs. [36, 37], by adding the following mass-like term to the chiral Lagrangian:

$$\Delta \mathcal{L}^{\text{DWF}} = -\frac{\mu f^2}{4} \text{Str}(\Sigma \Omega^\dagger + \Omega \Sigma^\dagger), \quad (26)$$

where Ω is a spurion which transforms as the mass matrix transforms, and in the end we set $\Omega = m_{\text{res}} \times I$. This leads to the familiar expression for the tree-level mass of a PGB

composed of two domain-wall quarks:

$$m_{xy}^2 = \mu(m_x + m_y + 2m_{\text{res}}). \quad (27)$$

Clearly this term will not contribute at leading order to B_K , since the Ω spurion transforms in the same manner as the mass spurion, and the mass term did not contribute at this order. Consequently, one may simply shift the valence quark masses by $m_{\text{val}} \rightarrow m_{\text{val}} + m_{\text{res}}$ in the results of this paper to transform them into expressions that apply to lattice simulations with domain-wall valence quarks and staggered sea quarks.³

Finally we must consider the fact that, while one constructs a lattice operator to correspond to a continuum operator with a particular spin, once on the lattice, this operator is allowed to mix due to gluon exchange with operators that correspond to other continuum spin structures. Lattice operator mixing patterns can become especially complicated when one introduces staggered quarks because now the desired lattice operator can not only mix with other operators with incorrect spins, but also those with incorrect tastes. Fortunately, in the mixed action theory that we consider here, the symmetry of the G-W valence sector is sufficient to prevent mixing between the lattice B_K operator and new operators with non-trivial taste structure. Because the valence quarks in the B_K four-fermion operator do not transform under taste symmetry, the B_K operator is clearly not in the same lattice symmetry irrep as any taste-violating four-fermion operators. Furthermore, in the case of pure G-W valence quarks, the B_K operator cannot mix with operators of the wrong chirality. In realistic simulations with domain-wall valence quarks, however, the desired lattice B_K operator with spin structure $VV + AA$ mixes with the undesired $VV - AA$ operator. Fortunately, this contamination from the $VV - AA$ lattice operator can be removed nonperturbatively using the standard method of Rome-Southhampton [22].

To summarize, the result of this spurion analysis is that the leading order operator that contributes to B_K in the mixed action case is simply the continuum operator naively gener-

³ It should also be noted that the Dirac mass parameter, m , which is the input for domain-wall lattice simulations, is not, in fact, the bare quark mass that should be used in χ PT expressions. Rather, the physical current quark mass is *proportional* to the Dirac mass parameter [28]. In the case of the noninteracting domain-wall theory, the constant of proportionality is a calculable function of the domain-wall height, M_5 : $m_{\text{phys}} = m M_5 (2 - M_5)$. In the interacting theory, however, this coefficient is unknown. Nevertheless, one can use the Dirac mass parameter in mixed action χ PT expressions and account for the unknown mass renormalization by allowing the parameter μ to be different in the valence and sea sectors.

alized to the mixed action theory. This is simpler than the full staggered case [23], in which many new operators appeared at leading order due to taste-symmetry breaking. Nevertheless, taste-symmetry breaking will still enter the mixed action calculation of B_K through the masses of PGBs in loop diagrams. In addition, taste-breaking operators will generate operators of next-to-leading order (NLO) in the chiral effective theory that will contribute to analytic terms; we will discuss these in Sec. III C.

B. Contribution of B_K at 1-Loop

Recall from Eq (16) that the kaon B-parameter is defined as the ratio $\mathcal{M}_K/\mathcal{M}_K^{\text{vac}}$. At tree-level,

$$\left(\frac{\mathcal{M}_K}{\mathcal{M}_K^{\text{vac}}}\right)^{\text{LO}} \equiv B_0. \quad (28)$$

Because all higher-order contributions to B_K are identically zero in the limit of massless quarks, this expression defines the B-parameter in the chiral and continuum limits.

At 1-loop, the $K^0 - \overline{K}^0$ matrix element receives contributions from the diagrams shown in Fig. 1, where we have specified the location of each of the two left-handed currents in the chiral operator \mathcal{O}_K^χ .⁴ This factorization of the operator is useful because the calculation of the kaon matrix element can then be separated into two pieces, the 1-loop corrections to f_K and the 1-loop corrections to B_K in which we are interested. In terms of the contributions from the diagrams in Figure 1, the B_K matrix element can be written as

$$\mathcal{M}_K = \frac{8}{3} B_0 f^2 m_{xy}^2 \{1 + X[\text{Figs. 1(b)-(c)}] + X'[\text{Figs. 1(d)-(f)}]\}, \quad (29)$$

where X and X' indicate the results of specific diagrams and m_{xy}^2 is the 1-loop kaon mass squared. At 1-loop, the form of $\mathcal{M}_K^{\text{vac}}$ is simple:

$$\mathcal{M}_K^{\text{vac}} = \frac{8}{3} m_{xy}^2 f_{xy}^2, \quad (30)$$

where m_{xy}^2 and f_{xy} are the 1-loop corrected values. It is clear that diagrams (b) and (c) in Fig. 1 factorize – the left-half of each diagram is the 1-loop correction to f_K , while the right

⁴ Note that this factorization is only possible at leading order. At higher orders, B_K receives contributions from operators which are not simply products of left-handed currents.

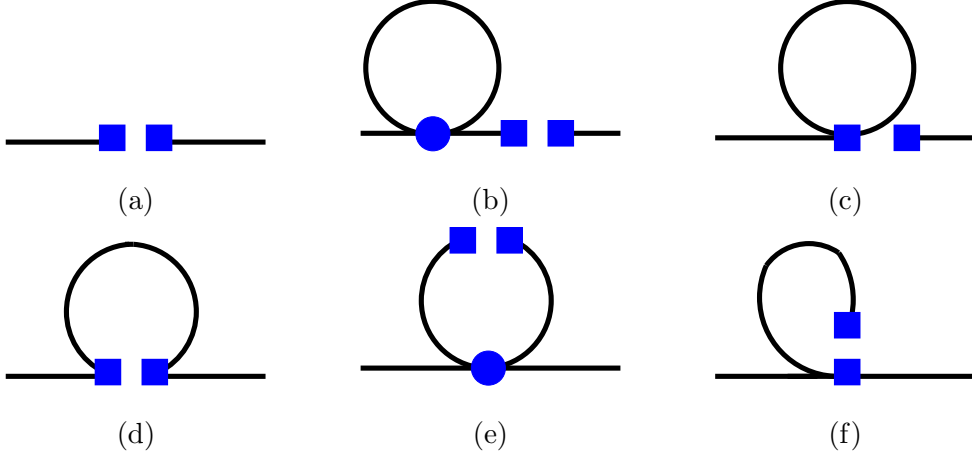


FIG. 1: Tree-level and 1-loop contributions to \mathcal{M}_K . The circle represents a vertex from the LO staggered chiral Lagrangian. Each square represents an insertion of one of the two left-handed currents in \mathcal{O}_K^X and “changes” the quark flavor from $d \leftrightarrow s$.

half is just f at tree-level. Mathematically,

$$X[\text{Figs. 1(b)-(c)}] = 2 \frac{\delta f_{NLO}}{f}, \quad (31)$$

where the factor of two comes from the fact that the loop can appear on either leg. Diagrams 1(b) and 1(c) therefore turn the leading order f^2 into the 1-loop f_{xy}^2 in Eq. (29):

$$\mathcal{M}_K = \frac{8}{3} B_0 f_{xy}^2 m_{xy}^2 + X'[\text{Figs. 1(d)-(f)}], \quad (32)$$

such that B_K at one loop only depends on diagrams 1(d)-(f):

$$B_K^{1\text{-loop}} = B_0 + \frac{3}{8} \frac{X'[\text{Figs. 1(d)-(f)}]}{f_{xy}^2 m_{xy}^2}. \quad (33)$$

Figure 2 shows the quark flow diagrams that correspond to the meson diagrams in Figs. 1(d)-(f). It is interesting to note that the only place where sea quarks appear in these diagrams is in the disconnected hairpin propagators of diagrams 2(b) and (c). In particular, there are no contributions from mixed mesons made of one sea and one valence quark, so the new parameter in the mixed action chiral Lagrangian, Δ_{Mix} , does not appear in B_K to 1-loop.

We now proceed to calculate the 1-loop contributions to B_K from Figure 2. The connected diagrams, 2(a), (d), and (e), combine to give the result

$$\mathcal{M}_{\text{conn}} = \frac{B_0}{6\pi^2} \int \frac{d^4 q}{(2\pi)^4} \left[\frac{2m_{xy}^4}{q^2 + m_{xy}^2} - \frac{m_X^2 + m_{xy}^2}{q^2 + m_X^2} - \frac{m_Y^2 + m_{xy}^2}{q^2 + m_Y^2} \right]. \quad (34)$$

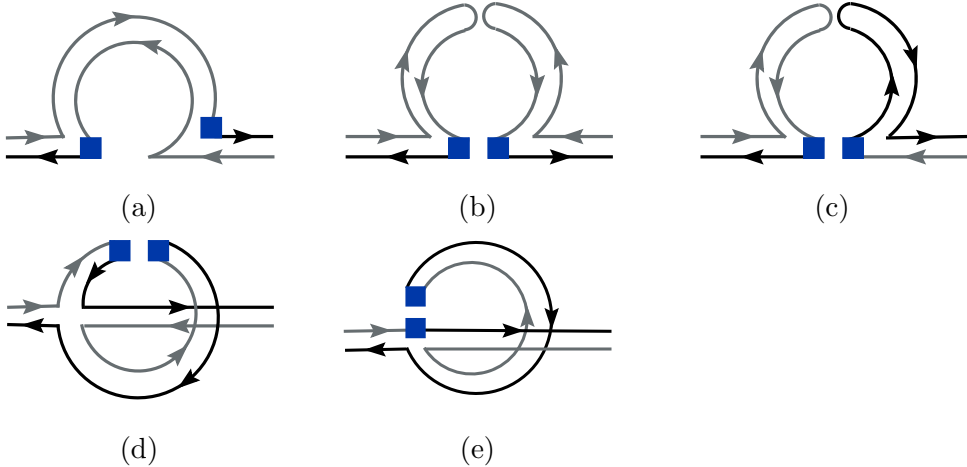


FIG. 2: Quark flow diagram contributions to B_K at 1-loop. One external meson is a \bar{K}^0 and the other is a K^0 . The two boxes represent an insertion of the B_K operator. Each box “changes” the valence quark flavor from $d \leftrightarrow s$. Diagrams (a)–(c) contribute to Fig. 1(d), diagram (d) contributes to Fig. 1(e), and diagram (e) contributes to Fig. 1(f).

The contribution from the disconnected diagrams, 2(b) and (c), is somewhat more tedious to evaluate because of the double poles in the hairpin propagators:

$$\mathcal{M}_{disc} = \frac{2}{3} B_0 \int \frac{d^4 q}{(2\pi)^4} (m_{xy}^2 + q^2) \{ D_{xx}^I(q) + D_{yy}^I(q) - 2D_{xy}^I(q) \}, \quad (35)$$

where D_{ij}^I is the taste-singlet disconnected propagator of Eq (15). Making use of the identity [23],

$$D_{xx} + D_{yy} - 2D_{xy} = (m_X^2 - m_Y^2)^2 \frac{\partial}{\partial m_X^2} \frac{\partial}{\partial m_Y^2} \{ D_{xy} \}, \quad (36)$$

we get the following result for the disconnected piece in the “1+1+1” partially quenched theory:

$$\mathcal{M}_{disc}^{PQ,1+1+1} = \frac{B_0}{48\pi^2} (m_X^2 - m_Y^2)^2 \frac{\partial}{\partial m_X^2} \frac{\partial}{\partial m_Y^2} \left\{ \int \frac{d^4 q}{(2\pi)^4} \sum_j \frac{(m_{xy}^2 + m_j^2)}{(q^2 + m_j^2)} R_j^{[4,3]}(\{M_{XY,I}^{[4]}\}; \{\mu_I^{[3]}\}) \right\}, \quad (37)$$

where $R_j^{[4,3]}$ is the residue arising from the double pole in the disconnected propagator; $R_j^{[4,3]}$, $\{M_{XY,I}^{[4]}\}$, and $\{\mu_I^{[3]}\}$ are defined in Sec. III D.

To get the full expression for B_K at NLO, one must combine the 1-loop contributions with analytic terms that arise from tree-level matrix elements of higher-order operators:

$$B_K^{PQ} = B_0 + \frac{3}{8} \left(\frac{\mathcal{M}_{conn} + \mathcal{M}_{disc}}{f_{xy}^2 m_{xy}^2} + \text{analytic terms} \right). \quad (38)$$

We discuss the analytic terms in the following subsection.

C. Analytic contributions to B_K at NLO

Next-to-leading order analytic contributions to B_K come from tree-level matrix elements of NLO operators. In MAXPT, such terms can come from operators of the following order in the power-counting scheme:

$$\mathcal{O}(p_{\text{PGB}}^4), \mathcal{O}(a^2 p_{\text{PGB}}^2), \mathcal{O}(a^4), \mathcal{O}(m_q^2), \mathcal{O}(p_{\text{PGB}}^2 m_q), \mathcal{O}(a^2 m_q). \quad (39)$$

There are many such operators in the mixed action chiral Lagrangian, however, since it is not necessary to separate them in fits to numerical lattice data, we do not enumerate them all here. Instead we use symmetry arguments to restrict the possible linearly independent terms as in Ref. [23].

First we discuss those analytic contributions which are easiest to determine. One can immediately rule out contributions from operators of $\mathcal{O}(p_{\text{PGB}}^4)$ because such operators contain four derivatives, but tree-level matrix elements contain only two fields upon which they can act. One can also rule out contributions from $\mathcal{O}(a^4)$ operators because, at tree-level, they would produce terms without powers of masses in them, and the chiral symmetry of the valence sector requires that the kaon matrix element vanish in the chiral limit. Finally, all contributions from $\mathcal{O}(a^2 p_{\text{PGB}}^2)$ operators must be proportional to m_{xy}^2 because the derivatives must act on the two external kaons, giving a factor of p^2 which becomes m_{xy}^2 when the kaons are on-shell. This leads to the first analytic term: $c_1 a^2 m_{xy}^2$.

All of the analytic terms that are not proportional to powers of a^2 are the same as in the continuum partially quenched theory. The mass dependence of these terms can be determined using CPS symmetry [38], where C and P are the usual charge conjugation and parity reversal symmetries, respectively. In QCD, S corresponds to the exchange of d and s quarks, however, in the mixed action lattice theory, we must impose a symmetry under the interchange of x and y valence quarks instead: $x \leftrightarrow y, m_x \leftrightarrow m_y$. There are only two linearly independent $\mathcal{O}(m_q^2)$ terms allowed by this symmetry; we choose to write them in the forms $c_2 m_{xy}^4 \propto c_2 (m_x + m_y)^2$ and $c_3 (m_x - m_y)^2$. Operators of $\mathcal{O}(p_{\text{PGB}}^2 m_q)$ only contribute one new linear combination of masses: $m_{xy}^2 \text{Tr}(M_{\text{sea}})$, where M_{sea} is the $N_{\text{sea}} \times N_{\text{sea}}$ sea quark mass matrix.

Finally, operators of $\mathcal{O}(a^2 m_q)$ can be shown to give no new independent contributions. There are three possibilities for the quark mass dependence: $(m_x + m_y)$, $(m_x - m_y)$, and $\text{Tr}(M_{\text{sea}})$. The first term, $a^2(m_x + m_y)$, is already included in c_1 , the second, $a^2(m_x - m_y)$, is forbidden by CPS symmetry, while the last term, $a^2\text{Tr}(M_{\text{sea}})$, vanishes for the following reason. The factor $\text{Tr}(M_{\text{sea}})$ always comes from the operator $\text{Str}(\Sigma M^\dagger + M \Sigma^\dagger)$ when $\Sigma = 1$, so the only operators that can lead to contributions of the form $a^2\text{Tr}(M_{\text{sea}})$ are $\mathcal{O}(a^2)$ operators multiplying $\text{Str}(\Sigma M^\dagger + M \Sigma^\dagger)$. However, by chiral symmetry, the $\mathcal{O}(a^2)$ operators cannot generate tree-level contributions to \mathcal{M}_K . Therefore, the $a^2\text{Tr}(M_{\text{sea}})$ terms also vanish.

To summarize, the following analytic terms contribute to B_K at NLO:

$$[c_1 a^2 m_{xy}^2, \quad c_2 m_{xy}^4, \quad c_3 (m_X^2 - m_Y^2)^2, \quad c_4 m_{xy}^2 (m_{U_P}^2 + m_{D_P}^2 + m_{S_P}^2)] . \quad (40)$$

Note that we have re-expressed them in terms of meson masses, rather than quark masses, because those are what one measures in a lattice simulation.

D. Next-to-Leading Order B_K Results

In this section we present results for a “1+1+1” theory in which $m_u \neq m_d \neq m_s$ in the sea sector, for a “2+1” theory in which $m_u = m_d \neq m_s$ in the sea sector, and for a “full QCD”-like expression in which we tune the valence-valence meson masses equal to the taste-singlet sea-sea meson masses.

B_K at NLO in the 1+1+1 PQ theory is

$$\left(\frac{B_K}{B_0}\right)^{\text{PQ},1+1+1} = 1 + \frac{1}{16\pi^2 f_{xy}^2 m_{xy}^2} [I_{\text{conn}} + I_{\text{disc}}^{1+1+1}] + c_1 a^2 + c_2 m_{xy}^2 + c_3 \frac{(m_X^2 - m_Y^2)^2}{m_{xy}^2} + c_4 (m_{U_P}^2 + m_{D_P}^2 + m_{S_P}^2) . \quad (41)$$

The connected 1-loop contribution, I_{conn} , comes from evaluating the integral in Eq. (34):

$$I_{\text{conn}} = 2m_{xy}^4 \tilde{\ell}(m_{xy}^2) - \ell(m_X^2)(m_X^2 + m_{xy}^2) - \ell(m_Y^2)(m_Y^2 + m_{xy}^2), \quad (42)$$

while the disconnected contribution, I_{disc}^{1+1+1} , comes from evaluating the integral in Eq. (35):

$$I_{\text{disc}}^{1+1+1} = \frac{1}{3} (m_X^2 - m_Y^2)^2 \frac{\partial}{\partial m_X^2} \frac{\partial}{\partial m_Y^2} \left\{ \sum_j \ell(m_j^2) (m_{xy}^2 + m_j^2) R_j^{[4,3]}(\{M_{XY,I}^{[4]}\}; \{\mu_I^{[3]}\}) \right\} . \quad (43)$$

In the above expressions, ℓ and $\tilde{\ell}$ are integrals regulated using the standard $S\chi$ PT scheme [17, 18]:

$$\int \frac{d^4 q}{(2\pi)^4} \frac{1}{q^2 + m^2} \rightarrow \frac{1}{16\pi^2} \ell(m^2), \quad (44)$$

$$\int \frac{d^4 q}{(2\pi)^4} \frac{1}{(q^2 + m^2)^2} \rightarrow \frac{1}{16\pi^2} \tilde{\ell}(m^2), \quad (45)$$

One can completely account for lattice finite volume effects by turning the above integrals into sums. This yields an additive correction to the chiral logarithms [39]:

$$\ell(m^2) = m^2 \left(\ln \frac{m^2}{\Lambda_\chi^2} + \delta_1^{FV}(mL) \right), \quad \delta_1^{FV}(mL) = \frac{4}{mL} \sum_{\vec{r} \neq 0} \frac{K_1(|\vec{r}|mL)}{|\vec{r}|} \quad (46)$$

$$\tilde{\ell}(m^2) = - \left(\ln \frac{m^2}{\Lambda_\chi^2} + 1 \right) + \delta_3^{FV}(mL), \quad \delta_3^{FV}(mL) = 2 \sum_{\vec{r} \neq 0} K_0(|\vec{r}|mL) \quad (47)$$

where the difference between the finite and infinite volume result is given by $\delta_i^{FV}(mL)$, and K_0 and K_1 are modified Bessel functions of imaginary argument.

Finally, the residues and sets of meson masses that appear in the 1+1+1 disconnected contribution are defined to be:

$$R_j^{[n,k]}(\{m\}, \{\mu\}) \equiv \frac{\prod_{a=1}^k (\mu_a^2 - m_j^2)}{\prod_{i \neq j} (m_i^2 - m_j^2)}, \quad (48)$$

$$\begin{aligned} \{M_{XY,I}^{[4]}\} &\equiv \{m_X, m_Y, m_{\pi_I^0}, m_{\eta_I}\}, \\ \{\mu_I^{[3]}\} &\equiv \{m_{U_I}, m_{D_I}, m_{S_I}\}. \end{aligned} \quad (49)$$

and the mass eigenstates of the taste singlet flavor neutral PGB's in the 1+1+1 case are⁵

$$m_{\pi_I^0, \eta_I}^2 = \frac{1}{3} \left[m_{U_I}^2 + m_{D_I}^2 + m_{S_I}^2 \pm \sqrt{m_{D_I}^4 - (m_{U_I}^2 + m_{S_I}^2)m_{D_I}^2 + m_{S_I}^4 + m_{U_I}^4 - m_{S_I}^2 m_{U_I}^2} \right]. \quad (50)$$

The expression in the 2+1 case is somewhat simpler:

$$\begin{aligned} \left(\frac{B_K}{B_0} \right)^{\text{PQ,2+1}} &= 1 + \frac{1}{16\pi^2 f_{xy}^2 m_{xy}^2} [I_{\text{conn}} + I_{\text{disc}}^{2+1}] + c_1 a^2 + c_2 m_{xy}^2 \\ &+ c_3 \frac{(m_X^2 - m_Y^2)^2}{m_{xy}^2} + c_4 (2m_{D_P}^2 + m_{S_P}^2), \end{aligned} \quad (51)$$

⁵ Strictly speaking, in the case where $m_u \neq m_d$, the mass eigenstates of the flavor-neutral sector are not the same as the physical states, π_I^0 and η_I . Since the mixing between these two states is negligible (and vanishes in the isospin limit), usually one does not make a distinction between the mass eigenstates and the physical states.

where the connected term is the same as in the 1+1+1 case and the disconnected term is

$$I_{disc}^{2+1} = \frac{1}{3}(m_X^2 - m_Y^2)^2 \frac{\partial}{\partial m_X^2} \frac{\partial}{\partial m_Y^2} \left\{ \sum_j \ell(m_j^2) (m_{xy}^2 + m_j^2) R_j^{[3,2]}(\{M_{XY,I}^{[3]}\}; \{\mu_I^{[2]}\}) \right\}, \quad (52)$$

$$\begin{aligned} \{M_{XY,I}^{[3]}\} &\equiv \{m_X, m_Y, m_{\eta_I}\}, \\ \{\mu_I^{[2]}\} &\equiv \{m_{D_I}, m_{S_I}\}. \end{aligned} \quad (53)$$

When the up and down quark masses are degenerate, the flavor-neutral, taste-singlet mass eigenstates are:

$$\begin{aligned} m_{\pi_I^0}^2 &= m_{U_I}^2 = m_{D_I}^2, \\ m_{\eta_I}^2 &= \frac{m_{U_I}^2}{3} + \frac{2m_{S_I}^2}{3}. \end{aligned} \quad (54)$$

The disconnected term also becomes simple enough that we choose to show it explicitly:

$$I_{disc}^{2+1} = \frac{1}{3} (I_X + I_Y + I_\eta), \quad (55)$$

with

$$\begin{aligned} I_X &= \tilde{\ell}(m_X^2) \frac{(m_{xy}^2 + m_X^2)(m_{D_I}^2 - m_X^2)(m_{S_I}^2 - m_X^2)}{(m_{\eta_I}^2 - m_X^2)} \\ &\quad - \ell(m_X^2) \left[\frac{(m_{xy}^2 + m_X^2)(m_{D_I}^2 - m_X^2)(m_{S_I}^2 - m_X^2)}{(m_{\eta_I}^2 - m_X^2)^2} + \frac{2(m_{xy}^2 + m_X^2)(m_{D_I}^2 - m_X^2)(m_{S_I}^2 - m_X^2)}{(m_Y^2 - m_X^2)(m_{\eta_I}^2 - m_X^2)} \right. \\ &\quad \left. + \frac{(m_{D_I}^2 - m_X^2)(m_{S_I}^2 - m_X^2) - (m_{xy}^2 + m_X^2)(m_{S_I}^2 - m_X^2) - (m_{xy}^2 + m_X^2)(m_{D_I}^2 - m_X^2)}{(m_{\eta_I}^2 - m_X^2)} \right], \end{aligned} \quad (56)$$

$$I_Y = I_X (X \leftrightarrow Y), \quad (57)$$

$$I_\eta = \ell(m_\eta^2) \frac{(m_X^2 - m_Y^2)^2 (m_{xy}^2 + m_{\eta_I}^2)(m_{D_I}^2 - m_{\eta_I}^2)(m_{S_I}^2 - m_{\eta_I}^2)}{(m_X^2 - m_{\eta_I}^2)^2 (m_Y^2 - m_{\eta_I}^2)^2}. \quad (58)$$

Note that all of the sea quark dependence appears in the disconnected terms, and that these terms vanish for degenerate valence quark masses.

Multiple definitions of the “full QCD” point appear in the mixed action χ PT literature. This is because the mixed Ginsparg-Wilson valence, staggered sea theory has no true full QCD point at finite lattice spacing. Thus any choice of how to define the “full QCD” point

should be made for convenience. In this paper, we consider the two cases that most closely resemble the full unquenched theory.

One possible way to define “full QCD” for the mixed action theory with 2+1 flavors is to set $m_X = m_{D_I} = m_{\pi_I^0}$ and $m_Y = m_{S_I}$. On the lattice, this is nontrivial because it requires a tuning of the bare valence masses in order to set the valence PGB masses to be those of the taste-singlet sea PGB masses. This definition has the advantage, however, that the NLO expression for B_K looks very much like the continuum expression, except for the analytic term proportional to a^2 . In this case, the expression for B_K at NLO reduces to

$$\begin{aligned} \left(\frac{B_K}{B_0}\right)^{\text{“full”}} &= 1 + \frac{1}{16\pi^2 f_{xy}^2 m_{xy}^2} \left[2m_{xy}^4 \tilde{\ell}(m_{xy}^2) + \frac{1}{2}(m_X^2 - 7m_{xy}^2)\ell(m_{\eta_I}^2) - \frac{1}{2}(m_X^2 + m_{xy}^2)\ell(m_X^2) \right] \\ &+ \tilde{c}_1 a^2 + c_2 m_{xy}^2 + c_3 \frac{(m_X^2 - m_Y^2)^2}{m_{xy}^2} + \tilde{c}_4 (2m_X^2 + m_Y^2), \end{aligned} \quad (59)$$

where we have used the relationship $m_{\eta_I}^2 = (4m_{xy}^2 - m_X^2)/3$ which holds in this limit.⁶ This clearly approaches the standard result as $a \rightarrow 0$.

A more naive way to define “full QCD” in MAXPT is simply to set the bare valence quark masses equal to the bare sea quark masses. For perfect G-W valence quarks, this implies that the valence-valence meson mass equals the pseudoscalar taste sea-sea meson mass with the same quark content (*e.g.*, $m_K^{\text{val}} = m_{K_5}^{\text{sea}}$). This result differs from the one above by terms of order a^2 , and the resulting formula is not so simple. It is more convenient, however, in lattice simulations because it does not require any tuning of the bare masses. This is the definition of “full QCD” that we adopt for the numerical analysis in the following section.

IV. NUMERICAL ILLUSTRATION OF MIXED ACTION CONTRIBUTIONS TO B_K

We plan on carrying out a mixed action numerical simulation of B_K using domain wall fermions on the publicly available MILC improved staggered ensembles; we therefore use the known parameters and previous measurements on these lattices in order to obtain numerical error estimates for B_K using our χPT results. Currently there are two lattice spacings with large statistics on these ensembles, the “coarse” MILC lattices with $a \approx 0.125$ fm and

⁶ Note that the coefficients \tilde{c}_1 and \tilde{c}_4 are different than those in Eqs. (41) and (51) because the mass-squared of the taste-pseudoscalar meson and of the taste-singlet meson differ by a contribution of $\mathcal{O}(a^2)$.

the “fine” lattices with $a \approx 0.09$ fm. In this section we examine the modifications to the continuum expression for B_K that appear due to finite lattice spacing effects; these include both taste-breaking errors from the staggered sea sector and finite volume errors.

The NLO expression for B_K in a mixed action theory with $2 + 1$ flavors of sea quarks is given in Eq. (51). Discretization errors lead to two contributions – the shift in the mass-squared of the taste-singlet sea-sea meson that appears in the 1-loop disconnected contribution and the analytic term proportional to a^2 . Because we cannot *a priori* know the value of the coefficients of the analytic terms, and because the $\mathcal{O}(a^2)$ analytic term does not arise purely from taste-violating operators, we will neglect analytic terms in this numerical analysis of the size of taste-breaking contributions in B_K . We choose to study discretization errors on the $a \approx 0.125$ fm “coarse” MILC lattices since taste violations will be more pronounced than on the $a \approx 0.09$ fm lattices. In particular, we use the parameters of the ensemble with the lightest up and down sea quark masses on the smaller volume ($L/a = 20$); this ensemble has a light quark mass of $am_l^{\text{sea}} = 0.007$ and a strange quark mass of $am_s^{\text{sea}} = 0.05$.

In order to estimate the size of discretization errors in B_K we calculate the percent difference between the 1-loop contributions to B_K with and without taste-breaking:

$$\eta = \frac{B_K^{\text{1-loop}}(m_l^{\text{val}}, a^2 \Delta_I) - B_K^{\text{1-loop}}(m_l^{\text{val}}, 0)}{B_K^{\text{1-loop}}(m_l^{\text{val}}, 0)} . \quad (60)$$

In this expression we have set the heavier valence bare quark mass to be equal to the sea strange bare quark mass so that η is a function of the light valence quark mass, m_l^{val} , and the taste-singlet splitting, $a^2 \Delta_I$. The taste singlet meson is the heaviest of all of the staggered sea-sea mesons, and $a^2 \Delta_I$ is approximately $(450 \text{ MeV})^2$ on the coarse lattices. Because the only sea-sea mesons that contribute to the B_K at 1-loop in the mixed action theory are taste-singlets, this large splitting makes the effective sea quark mass considerably larger than a nominal light sea quark mass of $m_s/10$ or $m_s/7$ would suggest. On the fine lattices this splitting is much less, close to $(150 \text{ MeV})^2$, and this shows that it is necessary to approach the continuum limit in order to approach the chiral limit in the sea sector. Note, however, that the sea quark dependence is predicted to be small in the non-analytic contribution to our formulas. The sea quarks only contribute to the disconnected hairpin diagrams in B_K , and this is only around 15% of the connected piece at the physical point. It will, however,

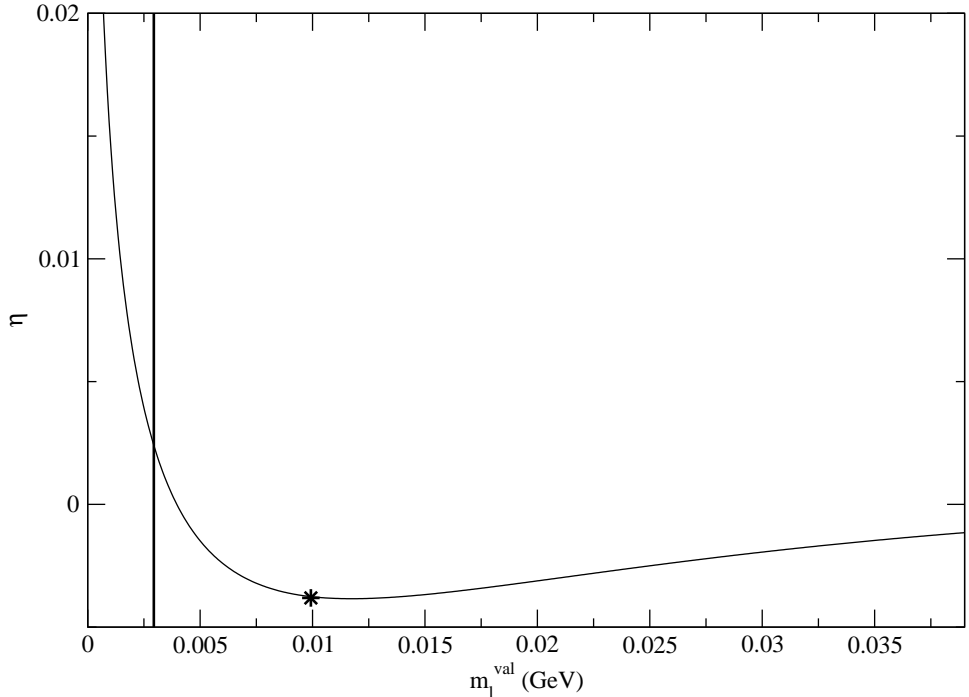


FIG. 3: Percentage difference between the 1-loop contributions to B_K with and without taste-breaking discretization errors, Eq. (60), as a function of valence light quark mass. The star corresponds to the “full QCD” point, while the vertical line shows the physical light quark mass.

be necessary to study the numerical data in order to determine the size of the analytic contribution, as well as to test the validity of our χ PT formulas at the physical strange quark mass.

We plot the percent difference, Eq. (60), as a function of valence quark mass in Fig. 3, setting $a^2\Delta_I$ to be the value measured in MILC simulations on the coarse lattices [11]. In this plot the star is the “full QCD” point defined by setting the bare valence and sea quark masses to be equal, while the vertical line shows the location of the physical value of the average up/down quark mass, $m_l^{\text{phys}} \approx m_s/27$. One can see that for larger valence light masses, η rapidly goes to zero. This is to be expected as the difference between the mass-squared of purely valence and purely sea mesons will ultimately be negligible for sufficiently large quark masses. At quark masses near or below the “full QCD” point, η begins to increase as the valence light mass decreases, such that as $m_l^{\text{val}} \rightarrow 0$, the percent difference blows up rapidly. Note, however, that this does not begin to happen until below the physical mass, so in the region of interest the error coming from taste violations is never higher than

0.5%. Note also that this estimate depends upon the value of the cutoff, Λ_χ , used (Fig. 3 uses $\Lambda_\chi = 1\text{GeV}$), although any cutoff dependence can be absorbed into the analytic terms which are not included in this numerical analysis.

We now repeat the above analysis, but include errors due to the finite spatial extent of the lattice. Such finite volume effects can be quite noticeable at the lightest sea quark masses available on the MILC configurations. One might imagine that the finite volume effects in the mixed case would not be very different than the continuum case, since the taste violating effects only enter through the taste singlet meson, which has a large mass. In actuality, this is precisely where there could be a problem, since the heavy singlet mass appears only in the sea sector. Partially quenched pathologies begin to appear when $m_\pi^{\text{val}} < m_\pi^{\text{sea}}$.⁷ Consequently, if the sea mesons are significantly heavier than the valence mesons (as they are in the mixed action theory) these pathologies may become more pronounced. We will see that this is, in fact, the case.

In analogy with Eq. (60), we define η_{FV} to be the percent difference between the 1-loop contribution to B_K in the mixed theory at finite volume and B_K in the mixed theory at infinite volume, both including discretization errors:

$$\eta_{FV}(m_l^{\text{val}}, a^2\Delta_I) = \frac{B_K^{1\text{-loop},\text{FV}}(m_l^{\text{val}}, a^2\Delta_I, L) - B_K^{1\text{-loop}}(m_l^{\text{val}}, a^2\Delta_I)}{B_K^{1\text{-loop}}(m_l^{\text{val}}, a^2\Delta_I)} . \quad (61)$$

We evaluate the above expression at a spatial lattice size of $L = 20$; the remaining parameters are the same as in the previous analysis. We then plot in Fig. 4 two curves – the dashed curve shows the percent difference in Eq. (61) for the continuum limit, $\eta_{FV}(m_l^{\text{val}}, 0)$, while the solid curve shows the same percent difference with $a^2\Delta_I$ set to its value on the coarse MILC lattices. Again, the star corresponds to the “full QCD” point and the vertical line indicates the physical light quark mass.

One can see that, for the “full QCD” point and larger masses, the error associated with finite volume effects, while not negligible, is quite small, of $\mathcal{O}(1\%)$ or less. Although the continuum and finite lattice spacing cases are different, in each instance finite volume effects are small. As the valence light quark mass drops below the sea light quark mass, the error shoots up rapidly, which is expected because quenching artifacts (where finite volume effects are more pronounced) become more noticeable in this region. As discussed above, the mixed

⁷ See, for example, Ref. [41].

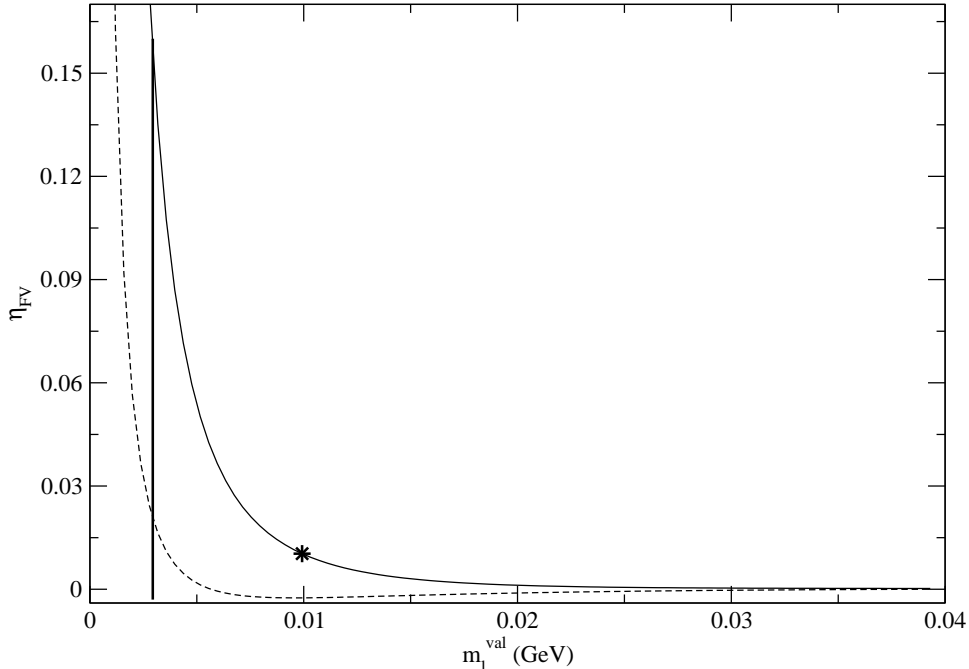


FIG. 4: Percentage difference in the 1-loop contributions to B_K in finite and infinite volume, Eq. (61), as a function of valence light quark mass. The dashed curve corresponds to η_{FV} with $a^2\Delta_I = 0$ (the continuum case), and the solid curve shows η_{FV} with $a^2\Delta_I$ set to its value on the coarse MILC lattices.

case sees these quenching artifacts at a larger valence mass, since the sea mesons are heavier. Although one might worry about this significant difference between the continuum and the mixed cases for the lighter masses (the difference is rather striking at the physical mass), this is not a practical problem. In actual lattice simulations, as the quark masses are lowered, the spatial volumes are also increased so as to keep the finite volume errors under control. For example, the MILC ensemble with a light sea quark mass of $am_l^{\text{sea}} = 0.005$ has a spatial length of $L = 24$ as opposed to 20 at the heavier masses. Thus Fig. 4 remains essentially unchanged, and the size of the percent error at the “full QCD” point (which is now at a lighter mass) should be roughly the same. The key point is that simulations are done to the right of this “wall” in Fig. 4 at which the error explodes, so one can correct for finite volume errors before performing extrapolations to the continuum and physical light quark mass.

V. CONCLUSIONS

In this work we have calculated the expression for B_K in a mixed action lattice theory with Ginsparg-Wilson valence quarks and staggered sea quarks to next-to-leading order in chiral perturbation theory. We have discussed in some detail how to extend the continuum calculation to the mixed action case, and we have provided expressions for both a “1+1+1” partially quenched theory ($m_u \neq m_d \neq m_s$) and a “2+1” partially quenched theory ($m_u = m_d \neq m_s$), both of which reduce to the corresponding partially quenched QCD expressions in the continuum limit.

It is illustrative to compare our expression for B_K in mixed action chiral perturbation theory to that for other lattice theories. Four parameters are needed to describe B_K in the continuum: one leading order constant, B_0 , and three NLO coefficients. In the case of pure Ginsparg-Wilson lattice fermions, the expression for B_K contains one additional coefficient proportional to a^2 . For domain-wall lattice fermions there is an additional constant, m_{res} , which comes from chiral symmetry breaking due to the finite domain wall separation. This term simply enters B_K as an additive shift to the quark mass and can be separately measured in a tree-level fit to the pion mass-squared. In the mixed action lattice theory with staggered sea quarks and domain wall valence quarks that we have considered here, taste-symmetry breaking effects produce an additive shift to the sea-sea meson mass squared. This is the only new term that appears in the calculation of B_K with domain-wall quarks on a staggered sea as compared to a pure domain-wall calculation. In contrast, the expression for B_K with staggered valence quarks on a staggered sea contains many new parameters, each of which must be determined from lattice simulations and subsequently removed in order to extract the value of B_K in the continuum. It is interesting to note that the expression for B_K in the mixed G-W, staggered lattice theory is no more complicated than that for a domain-wall simulation in which a different value of the domain-wall separation is used in the valence and sea sectors; such a “mixed” domain-wall simulation was previously proposed in Ref. [40]. In this case the value of m_{res} would differ in the valence and sea sectors, and the corresponding expression for B_K could be gotten from our expression, Eq. (41), by simply making the replacements $m_{\text{res}} \rightarrow m_{\text{res}}^{\text{valence}}$ and $a^2 \Delta_I \rightarrow m_{\text{res}}^{\text{sea}}$. Thus the taste-singlet sea-sea meson mass shift can be thought of as an effective m_{res} in the sea sector, though this effective “ m_{res} ” scales as a^2 , and consequently vanishes in the continuum limit.

Finally, we have presented a numerical analysis of the resulting expressions in which we have examined the size of discretization errors from taste-symmetry breaking in the sea sector and finite volume errors for the MILC coarse ($a \approx 0.125$ fm, $L=20$ and 24) lattice ensembles. We find that the non-analytic taste-breaking contributions to B_K in the mixed action theory are around 0.5% or less over the range of the extrapolation and so are quite small. The finite volume effects are somewhat larger for the mixed action case than in the continuum, but still remain at or below the 1%- level for the light quark masses used in the MILC ensembles. It will of course be necessary to study the numerical lattice data in order to determine the size of the analytic contribution, as well as to test the validity of our NLO χ PT formulas at the physical strange quark mass.

We believe that a lattice calculation of B_K using domain-wall valence quarks on top of improved staggered field configurations combines the best properties of both fermion discretizations. This method will give valuable cross checks on other established methods for calculating B_K , and ultimately it should give a useful constraint on the CKM matrix and phenomenology.

Acknowledgments

We thank Andreas Kronfeld, Donal O'Connell and André Walker-Loud for useful discussions and careful readings of the manuscript. We also thank the Institute for Nuclear Theory at the University of Washington for their hospitality while some of this work was completed. CA would also like to thank Norman Christ for useful discussions. This research was supported by the DOE under grant nos. DE-FG02-92ER40699 and DE-AC02-76CH03000.

- [1] C. T. H. Davies et al. (HPQCD), Phys. Rev. Lett. **92**, 022001 (2004), hep-lat/0304004.
- [2] C. Aubin et al. (MILC), Phys. Rev. **D70**, 114501 (2004), hep-lat/0407028.
- [3] I. F. Allison et al. (HPQCD), Phys. Rev. Lett. **94**, 172001 (2005), hep-lat/0411027.
- [4] E. Gamiz et al. (HPQCD) (2006), hep-lat/0603023.
- [5] J. Kim, T. Bae, and W. Lee, PoS **LAT2005**, 338 (2005), hep-lat/0510007.
- [6] S. D. Cohen, PoS **LAT2005**, 346 (2005), hep-lat/0602020.
- [7] M. Bona et al. (UTfit Collaboration), URL <http://utfit.roma1.infn.it/>.

- [8] J. Charles et al. (CKMfitter Group), URL <http://ckmfitter.in2p3.fr/>.
- [9] S. Eidelman et al. (Particle Data Group), Phys. Lett. **B592**, 1 (2004).
- [10] C. W. Bernard et al., Phys. Rev. **D64**, 054506 (2001), hep-lat/0104002.
- [11] C. Aubin et al., Phys. Rev. **D70**, 094505 (2004), hep-lat/0402030.
- [12] M. Creutz (2006), hep-lat/0603020.
- [13] C. Bernard, M. Golterman, Y. Shamir, and S. R. Sharpe (2006), hep-lat/0603027.
- [14] C. Bernard, M. Golterman, and Y. Shamir (2006), hep-lat/0604017.
- [15] Y. Shamir (2006), hep-lat/0607007.
- [16] W.-J. Lee and S. R. Sharpe, Phys. Rev. **D60**, 114503 (1999), hep-lat/9905023.
- [17] C. Aubin and C. Bernard, Phys. Rev. **D68**, 034014 (2003), hep-lat/0304014.
- [18] C. Aubin and C. Bernard, Phys. Rev. **D68**, 074011 (2003), hep-lat/0306026.
- [19] S. R. Sharpe and R. S. Van de Water, Phys. Rev. **D71**, 114505 (2005), hep-lat/0409018.
- [20] C. Aubin and C. Bernard (2005), hep-lat/0510088.
- [21] D. Verstegen, Nucl. Phys. **B249**, 685 (1985).
- [22] G. Martinelli, C. Pittori, C. T. Sachrajda, M. Testa, and A. Vladikas, Nucl. Phys. **B445**, 81 (1995), hep-lat/9411010.
- [23] R. S. Van de Water and S. R. Sharpe (2005), hep-lat/0507012.
- [24] W.-j. Lee and S. R. Sharpe, Phys. Rev. **D68**, 054510 (2003), hep-lat/0306016.
- [25] T. Becher, E. Gamiz, and K. Melnikov, Phys. Rev. **D72**, 074506 (2005), hep-lat/0507033.
- [26] P. H. Ginsparg and K. G. Wilson, Phys. Rev. **D25**, 2649 (1982).
- [27] D. B. Kaplan, Phys. Lett. **B288**, 342 (1992), hep-lat/9206013.
- [28] Y. Shamir, Nucl. Phys. **B406**, 90 (1993), hep-lat/9303005.
- [29] R. Narayanan and H. Neuberger, Phys. Lett. **B302**, 62 (1993), hep-lat/9212019.
- [30] R. Narayanan and H. Neuberger, Nucl. Phys. **B412**, 574 (1994), hep-lat/9307006.
- [31] R. Narayanan and H. Neuberger, Nucl. Phys. **B443**, 305 (1995), hep-th/9411108.
- [32] B. Bistrovic et al. (Lattice Hadron Physics), J. Phys. Conf. Ser. **16**, 150 (2005).
- [33] S. R. Beane, P. F. Bedaque, K. Orginos, and M. J. Savage (NPLQCD), Phys. Rev. **D73**, 054503 (2006), hep-lat/0506013.
- [34] O. Bar, C. Bernard, G. Rupak, and N. Shores, Phys. Rev. **D72**, 054502 (2005), hep-lat/0503009.
- [35] J. Bijnens, H. Sonoda, and M. B. Wise, Phys. Rev. Lett. **53**, 2367 (1984).

- [36] T. Blum et al., Phys. Rev. **D66**, 014504 (2002), hep-lat/0102005.
- [37] T. Blum et al. (RBC), Phys. Rev. **D68**, 114506 (2003), hep-lat/0110075.
- [38] C. Bernard, T. Draper, A. Soni, H. D. Politzer, and M. B. Wise, Phys. Rev. **D32**, 2343 (1985).
- [39] C. Bernard (MILC), Phys. Rev. **D65**, 054031 (2002), hep-lat/0111051.
- [40] M. Golterman and Y. Shamir, Phys. Rev. **D71**, 034502 (2005), hep-lat/0411007.
- [41] C. W. Bernard and M. F. L. Golterman, Phys. Rev. **D49**, 486 (1994), hep-lat/9306005.